From Magnesium Technology 2008, M.O. Pekguleryuz, N.R. Neelameggham, R.S. Beals, and E.A. Nyberg, Editors

Influence of Cerium on Texture and Ductility of Magnesium Extrusions

Raja K. Mishra[1], Anil K. Gupta[2], P. Rama Rao[3], Anil K. Sachdev[1], Arun M. Kumar[4] and Alan A. Luo[1]

[1] Materials and Processes Laboratory, General Motors Research & Development Center, Warren, MI, USA
[2] National Physical Laboratory, New Delhi, India
[3] International Advanced Research Centre for Powder Metallurgy and New Materials, Hyderabad, India.
[4] India Science Laboratory, General Motors Research & Development Center, Bangalore, India

Keywords: Magnesium, Texture, Extrusion, Cerium, Mechanical Properties.

Abstract

Unalloyed Mg and Mg-0.2%Ce alloy were extruded as solid rounds at 400°C in a 500 ton vertical extrusion press at 10 mm/sec. Tensile tests revealed a significant increase in elongation with only a small Ce addition of 0.2%. The addition of cerium caused a decrease in yield strength and an increase in work hardening delaying the onset of instability. EBSD analysis shows that the small Ce addition markedly alters the texture of the extruded rods during recrystallization, and orients the c-axes of the grains at an angle to the extrusion axis whereas they are mostly normal to the extrusion axis in Mg. This reorientation favors basal slip activity leading to higher elongation. While Mg deforms mainly by twinning and fracture initiates due to voids nucleating at twin intersections, the Mg-0.2Ce alloy shows void nucleation along nonintersecting shear bands parallel to the tensile axis. The results of this study point to a design approach that combines alloying and processing to alter the slip distribution which can enhance the formability of Mg alloys.

Introduction

Although the cost of magnesium has decreased dramatically in recent years [1], its use in wrought products like sheet and extrusions has been limited due to the poor workability of magnesium alloys in as cast, primary and subsequent fabrication stages [2]. While there are increasing attempts to enhance hot workability during extrusion, there is limited effort to improve the ductility of the primary fabricated material in the as-extruded or in the as-rolled conditions. Earlier efforts have alluded to the fact that alloying additions which can indeed change the crystal structure from HCP to BCC could be a promising approach [3], but these approaches have not found commercial acceptance since either large amounts of alloying are needed (17 a/o in the case of Li), or additions such as Be require special precautions. Recent approaches to increasing the extrudability and ductility of Mg alloys have been to explore the Mg-Al system, leading to the development of AM30 (Mg-3%Al) magnesium alloy [4]. This alloy shows better extrudability compared to AZ31 as well as improved room temperature ductility. However, both extrudability and formability are much lower than those routinely obtained for the workhorse AA6063 aluminum alloy used in the automotive industry. There is therefore a growing need for obtaining high formability wrought magnesium alloys for automotive applications [5]. However, what is not obvious is how to choose the alloying additions which accomplish the desirable effects.

Alloying behavior of metallic materials in regard to phase equilibria has been investigated by systematically determining binary, ternary and, in some cases, multi-component equilibrium diagrams. However, similar systematic studies of such alloying effects on deformation, forming and fracture behavior of Mg are far more demanding and have not been a research tradition. It is only through sporadic investigations that some understanding of alloying effects on Mg deformation has been gained. It is generally recognized that mechanical workability of Mg can be improved by alloying with Zn, Ca and certain RE elements [6-9]. This effect has been ascribed to a lowering of the critical resolved shear stress (CRSS) by alloying [8] resulting in changes to the microtexture during fabrication. The CRSS for prismatic slip in Mg at room temperature has been reported [10] to be about 100 times higher than that for basal slip. In contrast, Koike et. al. [11] have shown that the CRSS for <a + c> pyramidal slip and <a> prism slip at room temperature are merely 2.5 and 2.2 times that of <a> basal slip. If the difference in the CRSS of these slip systems can be further reduced, prismatic slip would offer two independent slip modes beyond the original two basal slip systems for a total of four, and pyramidal slip would offer four independent slip modes on its own [12], fulfilling the Taylor criterion of five independent slip systems to be available for general deformation. It is expected that this would increase the formability of Mg. Furthermore, if slip is easy, the effect of twinning can be minimized, and fracture can be delayed, making it also possible to have high ductility.

In one study, Barnett et. al. have speculated that addition of a small quantity of Ce to Mg reduces rolling forces by distributing deformation away from shear bands [13]. This can occur if Ce addition changes the CRSS values which in turn will alter the microtexture during hot forming. In the present study, we investigate the effect of a small amount of Ce on mechanical properties and microtexture in extruded rods. The microstructure-property relations for room temperature deformation of extruded Mg-0.2Ce are presented here and compared with those of extruded unalloyed Mg rods.

Experimental Procedure

Unalloyed Mg and Mg-0.2%Ce alloy melts of about 100 kg were prepared using commercially pure Mg ingots and Mg-20%Ce master alloy in a steel crucible with SF_6/CO_2 protective cover gas. Billets of 75 mm diameter and 230 mm length were cast at about 700°C into a permanent mold. The billets were preheated to 400°C for two hours and extruded in a Wellman Enefco™ 500-ton multipurpose vertical hydraulic press fitted with a circular die. Solid rods, approximately 15mm in diameter corresponding to an extrusion ratio of 25:1, were extruded using boron nitride lubricant at a billet speed of 10mm/sec and air cooled.

The samples for microstructural evaluation were obtained by scrapping the front 0.15 meters of the extruded rod where it had

attained a steady state of extrusion. Metallographic samples were prepared by standard methods, and the polished samples were etched in a solution containing 20 ml glacial acetic acid, 50 ml picric acid, 10 ml methanol and 10 ml de-ionized water. A Nikon™ optical microscope was used to record the microstructure in both longitudinal and transverse directions of the extruded rods. The polished samples were also examined by electron backscattered diffraction (EBSD) in a LEO™ 1450 scanning electron microscope operating at 20kV fitted with a TSL™ EBSD camera [14]. Detailed chemical mapping of Ce, Al, O, Mn and Mg were obtained from polished samples sectioned normal to the extrusion axis using a Cameca™ SX100 electron probe microanalyzer operating at 20 KV.

Tensile specimens with a 25 mm gauge length and 6.25 mm gauge diameter were machined from the extruded rods and pulled to failure in a Universal Testing Machine (Instron™, Capacity: 0-50 kN) at an average strain rate of 0.66×10^{-3}/s. At least three specimens were taken from different locations of the steady state portion of the extruded rod. Uniaxial compression tests were carried out in a United Testing FRM60™ machine equipped with a 27 ton (approx 250kN) load cell on 12.7 mm compressometer gauge on 37.4mm long samples machined to a diameter of 12.8 mm (length to diameter ratio of 3:1 to confirm to the ASTM E9 test procedure) to a maximum of 10% strain at a strain rate of 0.005/min.

Results

Smooth extrusions were obtained at an extrusion speed of 10 mm/s for both the materials. Fig. 1 shows typical microstructures obtained for Mg and the Mg-0.2%Ce alloy in the transverse direction. The micrographs from longitudinal sections are similar, showing no anisotropy in grain morphology. The morphology indicates a fully recrystallized and nearly equi-axed grain structure. Optical images taken from the mid-section of the deformed sample normal to the fracture surface (Fig. 2) show nearly equal amounts of twinned grains in both Mg and Mg-Ce samples, even though the fracture strain of the latter is over three times the former.

The room temperature tensile properties are listed in Table 1 and the actual tension plots are shown in Fig. 3. The tensile yield strength of Mg-0.2%Ce is about 35% lower than that of Mg. The stress-strain curve exhibits strain hardening behavior characteristic of slip dominated deformation. The most significant difference in the mechanical properties of the two samples is in the tensile ductility, which is substantially higher in Mg-Ce samples compared to that in Mg samples.

Fig. 4 shows electron microprobe maps of the Ce and O distribution taken from a polished surface of the Mg-0.2%Ce sample. Taken together, they show that Ce particles are associated with oxygen in many instances, suggesting that Ce forms a mixture of Mg-Ce intermetallics and oxide particles dispersed in the microstructure. A finite concentration (detection limit of the microprobe is ~0.1 wt%) of Ce was consistently observed in the matrix, away from particles. This could be either due to Ce in solution or particles of a Ce-Mg phase dispersed in the matrix. The larger intermetallic particles are distributed both inside the grains as well as on the grain boundaries, and their relative volume fraction was estimated to be about 1%.

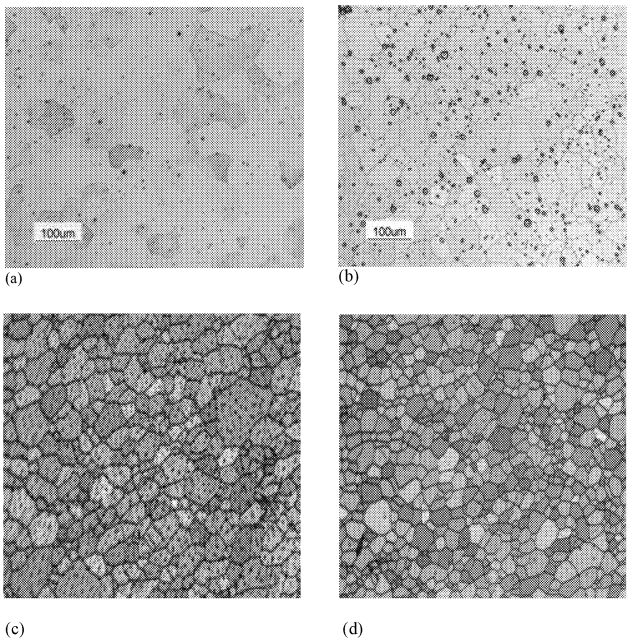

Fig 1. Optical micrographs and EBSD image quality maps of unalloyed magnesium (a,c) and Mg-0.2%Ce (b,d) following a 25:1 extrusion ratio. Average grain diameters are 34mm for Mg compared to 26mm for the Mg-0.2Ce alloy. Samples are taken normal to the extrusion direction.

The EBSD maps (inverse pole figure – IPF maps) in Figs. 5 (a) and (b) taken from transverse sections show that both materials have grains that have equiaxed shapes with straight boundaries, characteristic of a fully recrystallized extrusion. About 2% of the grains in the Mg-Ce alloy are twinned, but nearly none appear twinned in the unalloyed Mg samples. The average grain diameters measured from EBSD data are ~34 μm and 26 μm, respectively, for Mg and Mg-Ce samples after accounting for the twinned grains. The grain size measured with EBSD vis-à-vis by conventional method is being debated in the literature, and GM is currently part of a round robin measurement to create a new protocol by ASTM.

Table 1: Tensile, compression, and ductility values of Mg and Mg-0.2Ce alloys tested at room temperature

	Yield strength (tension), MPa	Yield strength (compression), MPa	UTS (tension), MPa	Total elongation (%)	n-value in tension based on hardening law of $\sigma = K\varepsilon^n$
Mg	106	53.5	155	9.1	0.24
Mg-0.2Ce	68.6	55.8	170	31	0.34

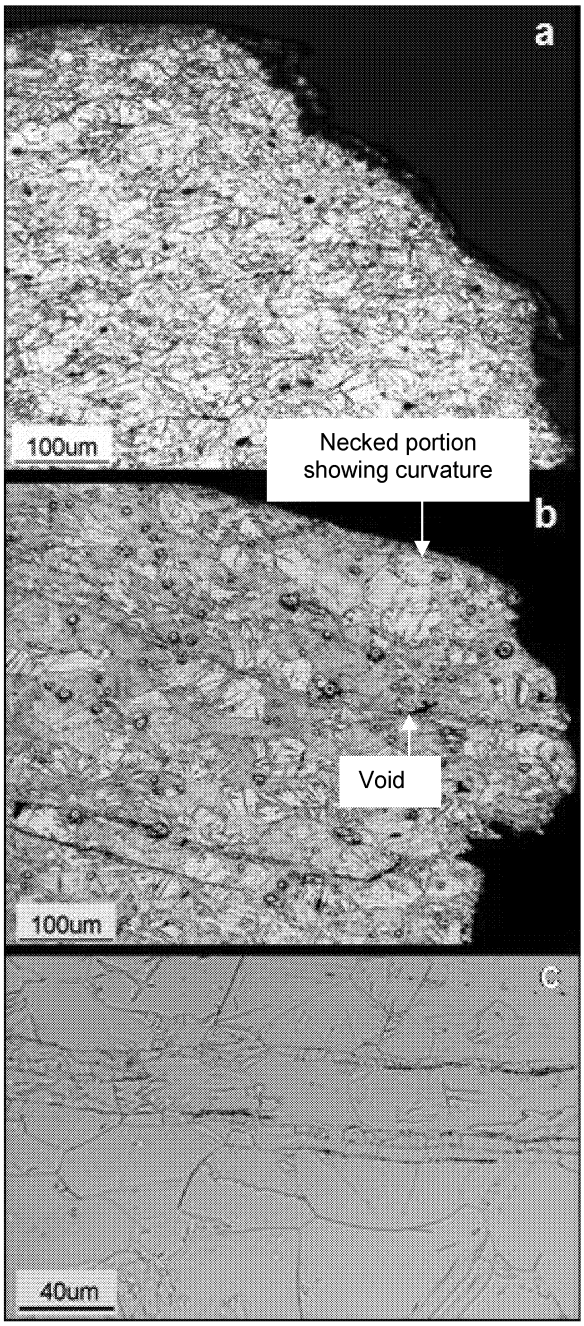

Fig 2. Optical micrographs taken from a cross-section normal and adjacent to the fracture surface. (a) Mg, (b) Mg-0.2Ce and (c) higher magnification on a shear band in (b). Note the curvature in (b) caused by necking of the sample which is absent in (a). Void formation close to a shear band is shown in (b).

The color distribution in the IPF maps (Figs. 5 (a) and (b)) show noticeable differences in the orientation of grains in the unalloyed Mg and Mg-0.2%Ce samples. While nearly all the grains are oriented with their basal planes parallel to the extrusion axis in the unalloyed Mg sample (basal plane normal perpendicular to the extrusion axis), this is not so in the Mg-Ce sample (note the higher proportion of red colored grains in Fig. 5(b) compared to Fig. 5(a)). The texture plots, with the axis of symmetry parallel to the extrusion axis for Mg and Mg-Ce samples in Figs. 5 (c) and (d), show the grains in Mg to have a perfect ring texture around the extrusion axis while the grains in Mg-Ce sample have their basal plane at an angle between 40 and 50 degrees to the extrusion axis. These textures translate to Schmid factors of over 0.4 in 56% of the grains in the Mg-Ce alloy compared to 36% of the grains in Mg, Fig. 6. The Taylor factor maps for the two microstructures show that over 80% of the grains in Mg have a Taylor factor of less than 1 compared to only 30% of such grains in the Mg-Ce sample. In other words, the Mg sample has a majority of grains in hard orientations for basal slip in contrast to the Mg-Ce alloy sample which has a large number of grains in a more formable orientation. An important effect of Ce, therefore, is to change the texture of the material drastically during recrystallization following extrusion.

Previous research has shown that a sharp initial texture and the polarity of deformation twins in magnesium lead to pronounced yield asymmetry associated with the activation of {10-12} twinning during extension (but not contraction) along the c-axis [15-17]. The compressive flow curves in Fig. 7 from Mg and Mg-Ce samples deformed along the extrusion axis show nearly identical compressive yield strength values in pure Mg and Mg-Ce samples. The threshold deformation required to nucleate the {10-12} extension twins in both samples is the same. However, the abrupt transition of pure Mg from elastic to plastic mode in compression is to be contrasted with the gradual transition in the Mg-Ce sample in Fig. 7. This behavior suggests that once twinning starts, the material deforms by twinning exclusively in pure Mg because of its texture, while in Mg-Ce samples, deformation proceeds with a combination of twinning and slip [14].

Fig. 8 shows fracture surfaces of tensile bars of Mg and Mg-0.2%Ce samples. In both cases, the fracture is intragranular. The cleavage planes are prominently observed inside the grains in the Mg samples that also contain evidence of void formation. In the Mg-Ce samples, on the other hand, no cleavage is seen. The dimples on the fracture surface of the Mg-Ce sample are demarcated by intense slip at the boundary region. Small particles inside the voids suggest particle-initiated fracture in the alloy. The difference in the nature of the fracture surfaces correlates well with the microstructure obtained from polished sections normal to the fracture surface in Fig. 2. Very little necking is noted in Mg in these sections compared to the Mg-Ce alloy. This is evident from the curved shape observed in the failed Mg-Ce sample (Fig. 2b). Crack initiation in the Mg sample can occur at twin intersections which can then propagate and expose twin planes successively to create the cleavage fracture surface appearance as in Fig. 8a. Mg-Ce sample in Fig 2b shows nonintersecting shear bands parallel to the tensile axis and void formation confined to the shear bands (Fig. 2b).

Discussion

The solubility of Ce in Mg is about 0.1% at 500ºC according to the phase diagram [18]. Any excess Ce will go to form intermetallics and oxide particles as was observed. The fully recrystallized grain structure in both samples suggests grain nucleation and growth to have been completed during cooling of

the extruded sample. The small amount of extension twins in the Mg-Ce alloys are most likely a result of compressive thermal stresses during cooling. The smaller grain size in the Mg-Ce alloy is believed to be due to the intermetallic particles that influence nucleation and growth of the recrystallized grains. A smaller grain size should result in an increase in YS due to the Hall-Petch effect [19]. Consequently, the lower YS observed in the Mg-Ce alloy could have been still lower if the alloy would have had a coarser grain size as in the unalloyed Mg sample.

A decrease in yield strength accompanied by an increase in ductile fracture toughness as a result of small solute additions has been noted in a few other instances. A notable example is the addition of Co to Fe where the scavenging of C in solid solution in the iron causes a reduction in the yield strength of the iron [20]. Somewhat similar results on the binary Mg-0.2Ce alloy presently obtained afford an opportunity for understanding their underlying cause.

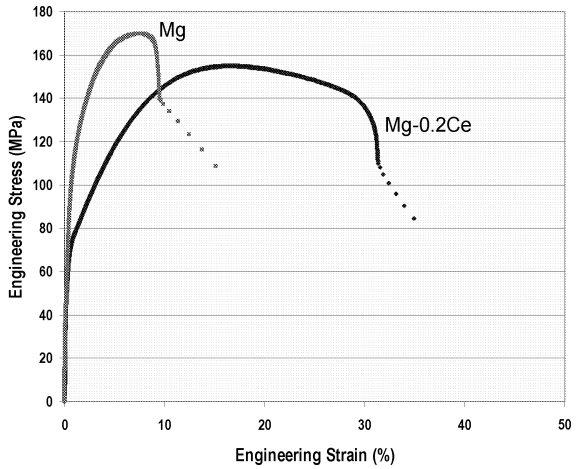

Fig 3. Tensile data for Mg (a) and Mg-0.2Ce (b) after extruding rods with a ratio of 25:1.

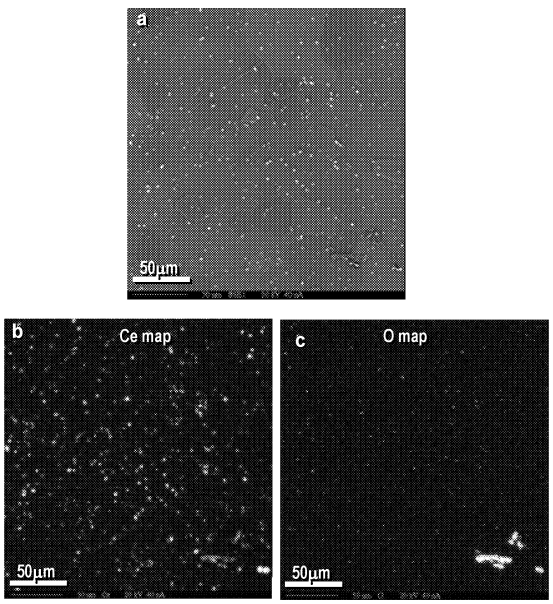

Fig 4. Microprobe analysis showing (a) backscattered image, (b) Ce distribution and (c) oxygen distribution in Mg-0.2%Ce alloy following an extrusion ratio of 25:1.

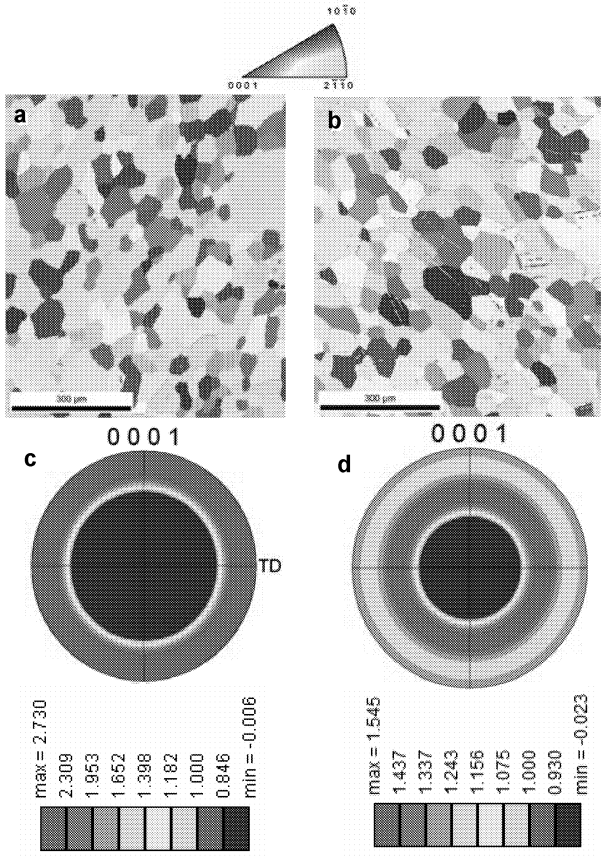

Fig 5. EBSD analysis and texture plots of fully recrystallized Mg (a and c) and Mg-0.2%Ce (b and d) following an extrusion ratio of 25:1.

The present study suggests that the reduction of tensile yield stress (Fig. 3) for Mg-Ce is due to an ease of basal slip because of favorably oriented grains. This feature is effectively precluded in Mg samples because of the unfavorable orientation of the grains for basal slip. Mg can deform by {10-11} twins (contraction) and {10-11} - {10-12} twins (double twins) in tension and it is expected that both samples will have an equivalent amount of these twins when the material has been deformed to high strains. This is reflected in the observations of a similar amount of twinning in both Mg and Mg-0.2Ce samples, Figs. 2 (a) and (b), with the essential difference between the two being the amount of slip in the latter sample, in addition to twinning.

Slip activity in the Mg-Ce sample is enhanced due to favorable grain orientation. The higher strain hardening coefficient of Mg-Ce extruded samples points to the ease of dislocation multiplication due to cross slip. The change in slip behavior due to Ce addition results in an increased capacity of the material for stored work in the shear bands. The suggestion pertaining to texture softening effect and redistribution of slip away from the shear bands during rolling of Mg-Ce alloys [13] needs to be rationalized with respect to the observation of shear bands and void formation. More studies are needed to understand the

interactions between Ce, shear band formation, associated texture changes and possible events that lead to localization, voids and failure as deformation proceeds.

It is the combination of lower yield strength and smaller grain size, accompanied by higher work hardening, changed slip distribution, and a texture favoring basal dislocation activity in the Mg-Ce sample, that gives it the high observed ductility. Since particle distribution can be changed by changing the amount of alloying additives as well as extrusion temperature and ratio, it is expected that grain size can be controlled through processing. The effect of Ce on the flow stress of different slip systems is not well known, but the current results suggest that Ce addition can potentially decrease the anisotropy of CRSS for different slip systems and increase the amount of dislocations in the material during deformation. Li additions have been shown to favor <c+a> dislocation activity in Mg that otherwise is predisposed to slip by basal dislocations [21]. A potential topic for future investigation can be to study if Ce addition to the Mg lattice changes the electronic charge distribution in the Mg lattice to alter the CRSS by reducing barriers to dislocation glide on all the slip systems.

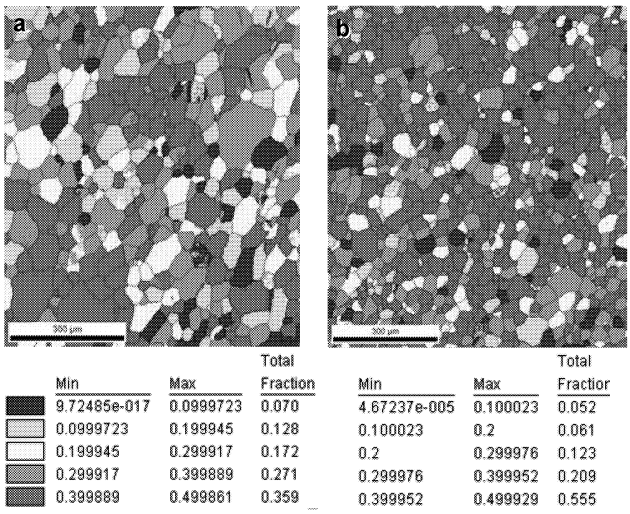

Fig 6. Schmid factor maps for basal slip for Mg (a) and Mg-0.2%Ce (b) following an extrusion ratio of 25:1.

Summary

The addition of only 0.2% Ce has demonstrated an unusual increase in the ductility of Mg. The Ce addition appears to favor the formation of recrystallized grains with their basal planes oriented at 40-50 degrees to the extrusion axis. The Mg-Ce alloy thus demonstrates an ease of basal slip which is effectively precluded in the extruded rods of Mg because a majority of the grains are oriented with their basal plane parallel to the extrusion axis. While twinning dominates Mg deformation, both twinning and slip activities occur in the Mg-Ce sample. The Ce addition also reduces the yield strength, refines the grain size and leads to a substantial increase in work hardening rate that delays the onset of instability. The change in deformation behavior manifests in different fracture behavior. A cleavage structure exposing twin surfaces is observed in unalloyed Mg due to cracks initiating at intersecting twin boundaries that subsequently interlink, while the fracture surface of the Mg-0.2Ce alloy exhibits a classical dimple structure as a result of slip accumulation and ductile tear.

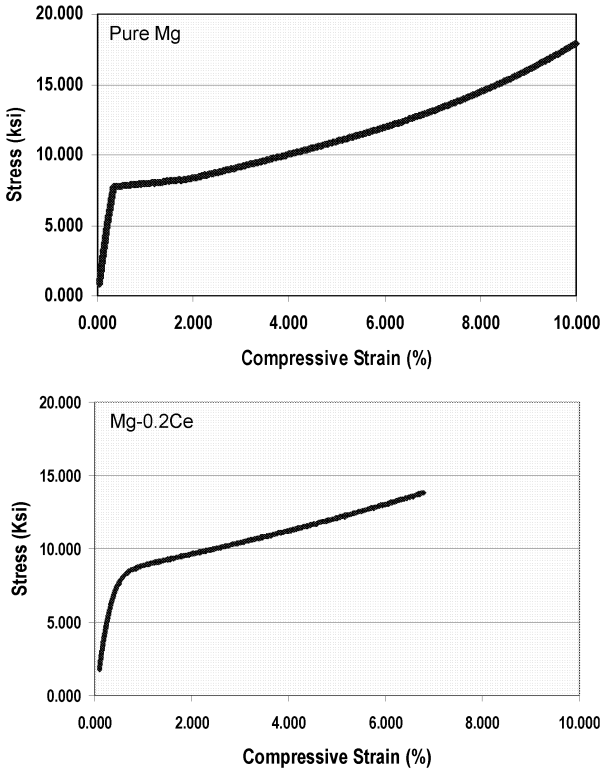

Fig 7. Compression data for pure Mg (a) and Mg-0.2Ce (b) after extruding rods with a ratio of 25:1

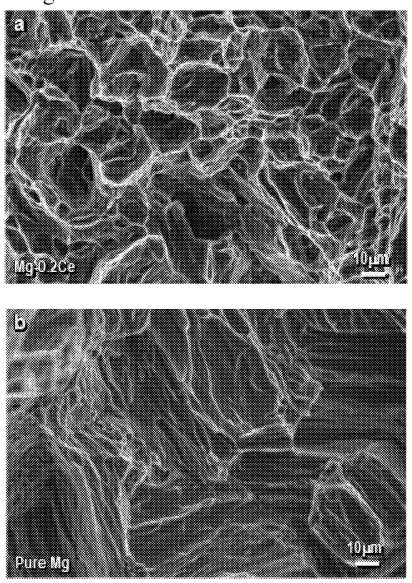

Fig 8. Fracture surface of tensile sample showing dimples characteristic of ductile intragranular fracture in Mg-0.2Ce alloy (a) and a mixture of dimples and cleavage planes in unalloyed Mg (b)

Acknowledgments

Dr. Gupta thanks General Motors for funding this project at the National Physical Laboratory. The authors gratefully acknowledge the help of Robert Kubic Jr. for EBSD data, Rick Waldo for microprobe data, Pinaki Biswas, Shashank Tiwari and S Vijayalakshmi for help with mechanical tests and microstructure.

References

1. D.A. Kramer, "Mineral Commodity Summaries – Magnesium Metal", United States Geological Survey, 2006.
2. Alan A. Luo, SAE 2005 Transactions - Journal of Materials and Manufacturing, SAE, Warrendale, PA, U.S.A., 411-421.
3. D. L. Olson, D. W. Wenman, V. I. Kaydanov, C. Suryanarayana and D. Eliezer, "The Search for Room Temperature Cubic Magnesium Alloys" in **Magnesium 2000**, eds. E. Aghion and D. Eliezer, Magnesium Research Institute (MRI) Ltd., Israel, 2000, pp165-172.
4. Alan A. Luo and Anil K. Sachdev, "AM30 – A New Wrought Magnesium Alloy", in Magnesium Technology 2007 Symposium, TMS Annual Meeting, (2007), Orlando, Florida, USA.
5. H. Dieringa, J. Bohlen, N. Hort, D. Letzig, K.U. Kainer, "Advances in Manufacturing Processes for Magnesium Alloys", Magnesium Technology 2007, eds. R.S. Beals, A.A. Luo, N.R. Neelameggham and M.O. Pekguleryuz, TMS, Warrendale, PA, (2007).
6. P. Menzen, **The Technology of Magnesium and Its Alloys**, A. Beck (ed), F. A. Hughes and Co. Ltd., London, (1940), 34.
7. J. C. McDonald, Trans. Metall. Soc. AIME, 212, (1958), 45
8. S. L. Couling, J. F. Pashak and L. Sturkey, Trans. ASM, 51, (1959), 94
9. B. C Wonsiewicz and W. A. Backofen, Trans. Metall. Soc. AIME, 239, (1967), 1422.
10. S. E. Ion, F. J. Humphreys, S. H. White, Acta Metall. 30, (1982),1909.
11. J. Koike, T. Kobayashi, T. Mukai, H. Watanabe, M. Suzuki, K. Maruyama, K. Higashi, Acta Mater. 51, (2003), 2055.
12. S. R. Agnew, O. Duygulu, Int. J. Plasticity. 21, (2005), 1161.
13. M. R. Barnett, M. D. Nave, and C. J. Bettles, Materials Science and Engineering, A386, (2004), pp205-211.
14. L. Jiang, J. J. Jonas, R. K. Mishra, A. A. Luo, A. K. Sachdev and S. Godet Acta Materialia, 55, (2007), 3899-3910.
15. E.W. Kelley and W.F. Hosford, Trans. TMS-AIME, 242, (1968), 5.
16. E.A. Ball and P.B. Prangnell, Scripta Metall. Mater., 31, (1994), 111.
17. J. Koike, Metall Mater Trans A, 36, (2005), 1689.
18. C. S. Robert, **Magnesium and its Alloys**, Wiley, New York, (1960).
19. R Armstrong, I. Codd, R. M. Douthwaite and N. J. Petch, Phil Mag 7, (1962), 40.
20. M. Srinivas, G. Malkondaiah and P. Rama Rao, Proceedings of the Royal Society, London, (1994), 447, 223.
21. S. Ando, K. Nakamura, K. Takashima and H. Tonda, Mater. Trans., (1992), JIM, 42, 2845.